

Case Report

A craniopharyngioma in a Wistar rat most likely originated in a Rathke's cleft cyst

Laura Polledo^{1*}, Robert Kreutzer¹, Yoshimasa Okazaki¹, Tanja Razingger², and Klaus Weber²

¹ AnaPath GmbH, AnaPath Services, Hammerstrasse 49, 4410 Liestal, Switzerland

² AnaPath GmbH, Buchsweg 56, 4625 Oberbuchsiten, Switzerland

Abstract: We examined a 110-week-old RccHanTM: WIST Wistar male rat from a carcinogenicity study. No clinical signs were observed, and the rat was sacrificed at the end of the study. Macroscopically, within the midline of the sphenoid bone, was a 10 mm, non-infiltrative, soft, heterogeneous mass. Microscopic evaluation showed an expansile, cystic proliferation, consisting of two patterns of epithelial lining: well-differentiated areas lined by a single layer to a pseudostratified, ciliated-cuboidal epithelia with Goblet cells compatible with Rathke's cleft cyst; and poorly differentiated ones that formed irregular papillary projections, covered by atypical epithelia with squamous differentiation and hyperkeratosis compatible with areas of craniopharyngioma. Pleomorphisms were high in atypical areas with up to 2–3 mitotic figures per high power field. Within the cystic cavities, there was abrupt keratinization, mucus, cholesterol clefts, and foci of foamy macrophages. Immunohistochemistry revealed strong pancytokeratin immunolabelling of neoplastic cells confirming the epithelial origin. Well-differentiated epithelial lining showed cytokeratin-20 and cytokeratin-8 immunoreactivity, whereas the atypical squamous epithelium presented with a loss of cytokeratin-20 positive signal and weak to moderate positivity with cytokeratin-8. Areas compatible with a Rathke's cleft cyst and craniopharyngioma were considered to co-exist in the same mass. (DOI: 10.1293/tox.2019-0068; J Toxicol Pathol 2020; 33: 183–187)

Key words: craniopharyngioma, rat, Rathke's cleft cyst, pituitary gland, craniopharyngeal duct, cytokeratin

A 110-week-old RccHanTM: WIST Wistar, male rat from a 104-week repeated-dose feeding carcinogenicity study, was examined. This animal belonged to the low dose group, and was sacrificed at the end of the treatment. The in-life phase of the study was conducted at Harlan Laboratories Ltd. in Switzerland. The study was approved by the Animal Experimentation Ethics Committee and was performed in an AAALAC-accredited laboratory following the Swiss Animal Protection Law. All experimental procedures and facilities complied with the requirements of Directive 2010/63/EU and the appropriate national legislation. The animals were kept under standard conditions, and the in-life observations of a standard long-term carcinogenicity study were performed. The rat was received routine necropsy and histopathological examination according to the study schedule. In addition to routine HE, sections from the mass were stained by Masson-trichrome (MT) and Periodic Acid-Schiff (PAS). Immunohistochemical studies were performed on additional sections of the lesion using anti-pancytokeratin

(PanCK, polyclonal rabbit antibody, Abcam, Cambridge, UK, ab9377, dilution 1:5), Anti-cytokeratin 20 (CK20, polyclonal rabbit antibody, Abcam, ab118574, dilution 1:50) and anti-cytokeratin 8 (CK8, polyclonal rabbit antibody, Abcam, ab59400, dilution 1:50). NovoLink Polymer (NovoLinkTM Max Polymer Detection System (RE7280-K) was used for immunological binding, and DAB-Substrat-Chromogen-Mix with hematoxylin counterstaining was used for color development. The IHC technique was checked for quality control with validated positive and negative controls.

We did not observe abnormal features, clinical signs, or weight loss (final body weight was 634 g) in the present case. No macroscopic findings were found during necropsy except an intracranial 10 mm, soft, round, non-infiltrative, heterogeneous mass that was found in the sagittal line lying on the sphenoid bone (corresponding to the pituitary region) and compressing the overlying base of the brain. Microscopic evaluation of the mass showed a highly heterogeneous, circumscribed, partially encapsulated, expansile, and cystic epithelial tumor (Fig. 1). Cystic cavities were lined by two different patterns of epithelial growth: in well-differentiated areas, the epithelium resembled the Rathke's cleft lining. In poorly differentiated areas, there was atypical squamous epithelium with marked hyperkeratosis. The well-differentiated epithelial lining was a single to pseudostratified layer of ciliated-cuboidal cells (Fig. 2A and B), with the presence of PAS-positive Goblet cells (Fig. 2C). These cells were polygonal, up to 40 µm, abundant, eosinophilic, with distinct

Received: 2 September 2019, Accepted: 16 March 2020

Published online in J-STAGE: 3 April 2020

*Corresponding author: L Polledo (e-mail: lpolledo@anapath.ch)

©2020 The Japanese Society of Toxicologic Pathology

This is an open-access article distributed under the terms of the Creative Commons Attribution Non-Commercial No Derivatives

(by-nc-nd) License. (CC-BY-NC-ND 4.0: <https://creativecommons.org/licenses/by-nc-nd/4.0/>).



cytoplasm, and round nuclei with coarse chromatin and 1–2 variably sized nucleoli. Poorly differentiated areas presented with 1 to 3-cell layers of atypical squamous epithelium, with intratumorally invasive neoplastic cells arranged in irregular papillary projections (Fig. 2D and E), supported by abundant fibrous stroma. Often, there was stratified epithelium that appeared spongy (Fig. 2F). Cellular pleomorphism was high in atypical areas, and anisokaryosis and anisocytosis were also marked. There were 2–3 mitotic figures per high power field ($\times 400$) (Fig. 3A). Cystic cavities were mostly replete by abrupt laminar orthokeratotic hyperkeratosis, characterized by the presence of anuclear flakes of keratin. Admixed with it, there was abundant pale blue mucus and multifocal deposits of lesser amounts of an eosinophilic, proteinaceous substance. Keratin and mucus stained red and pale blue, respectively, with MT and both stained strongly pink with PAS, (Fig. 3B). Within the cystic cavities, there was also a multifocal accumulation of cholesterol clefts and clusters of foamy macrophages (Fig. 3C) which often contained hemosiderin. Within the stroma, there was a moderate inflammatory infiltrate of lymphocytes, macrophages, and plasma cells. No areas of calcification were detected. The overlying brain was slightly deformed by the mass pressure, with signs of local pressure atrophy, but with no evident tumoral invasion. Remnants from the pituitary gland and nasal cavity were studied in detail for further lesions, but no changes were noted, and there was no evidence of any other tumors in other distant organs. No lesions related to this tumor were found in any rats of the original long-term study; therefore, this lesion was considered to have spontaneously developed.

The atypical and highly proliferative epithelium were characteristic of epithelial neoplasia. Given its location, the compression of the brain, and the presence of papillary projections lined by squamous epithelium with hyperkeratosis, the diagnosis was compatible with a craniopharyngioma (CP)¹. Additional features such as the spongy squamous epithelium and the presence of cholesterol are frequently observed in CPs in humans². However, to the authors' best knowledge, these have not been described in rats.

The available literature regarding the immunohistochemistry profile of CPs in rats is limited to immunolabelling with a panCK antibody in CPs³. In the present case, there was a clear immunoreactivity with panCK of the cyst lining, confirming the epithelial origin (Fig. 3D). Additionally, CK20 and CK8 immunohistochemistries were performed, based on suspicion of a proliferation derived from embryonic epithelial remnants of the craniopharyngeal duct. CK20 is the preferential marker in humans to differentiate CP from Rathke's cleft cyst (RCC) as CPs do not express CK20 in contrast to RCC, being that CK8 is usually positive in both^{4–8}. The well-differentiated areas resembling Rathke's cleft epithelium show CK8 and CK20 immunoreactivity, compatible with RCC⁹. By contrast, poorly differentiated areas of squamous epithelium show no to weak CK20 positive signals (Fig. 3E) and variable immunolabelling for CK8 (Fig. 3F), compatible with a CP. Further,

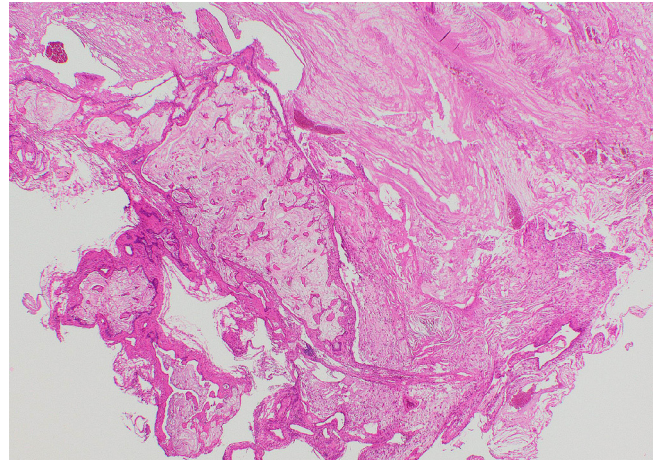


Fig. 1. Hematoxylin and eosin staining of the cystic mass. The mass was a cystic epithelial tumor containing mucus, keratin, and cholesterol clefts. The cysts were lined by two different patterns of epithelial growth: well-differentiated areas of the epithelium resembling Rathke's cleft lining; and areas lined by poorly atypical squamous epithelium with marked hyperkeratosis. Magnification: $\times 20$.

the keratin from hyperkeratotic areas had strong immunolabelling against panCK and CK8, and weak immunolabelling for CK20. Therefore, areas of RCC and CP were considered to co-exist in the same mass.

RCCs are benign epithelial cystic expansions of primitive vesicles from the craniopharyngeal duct¹⁰, with an incidence rate below 1% in rats^{11,12}. Histologically, RCCs appear as simple round cysts or as a large primary cyst surrounded by a cluster of smaller secondary cysts lined mainly by a single-layer of squamous, cuboidal, or ciliated epithelium. This epithelium normally contains PAS-positive proteinaceous fluid and is situated between the *pars intermedia* and the *pars distalis*⁹. CPs are epithelial, slow-growing, expansile tumors within the sellar region, histologically benign, but tend to be clinically aggressive due to mass-effect compression of the pituitary gland or adjacent brain tissue^{2,13,14}. CPs are rarely found in animals (reported only in rodents, dogs, and cats) or humans (mostly in children). In rats, the incidence is reported to be less than 1%^{3,12,15–18}.

CPs and RCCs both originate in Rathke's pouch, and therefore arise from a common epithelial lining: cuboidal, ciliated epithelium, often containing mucus and goblet cells^{1,19}. Histopathology is one of the most reliable tools for differential diagnosis; however, differentiating among RCCs and CPs can be challenging as some of the histological features overlap⁸. The predominance of squamous epithelium with papillary tumor growth and cyst formation with marked hyperkeratosis—as is observed in some areas in the studied mass—suggests a diagnosis of CP^{7,20,21}. Furthermore, RCCs and CPs have been hypothesized to represent two poles of a pathological spectrum derived from the craniopharyngeal duct, from RCCs to CP^{2,5,7,8,22}. In this study, coexistent areas that were histologically compatible

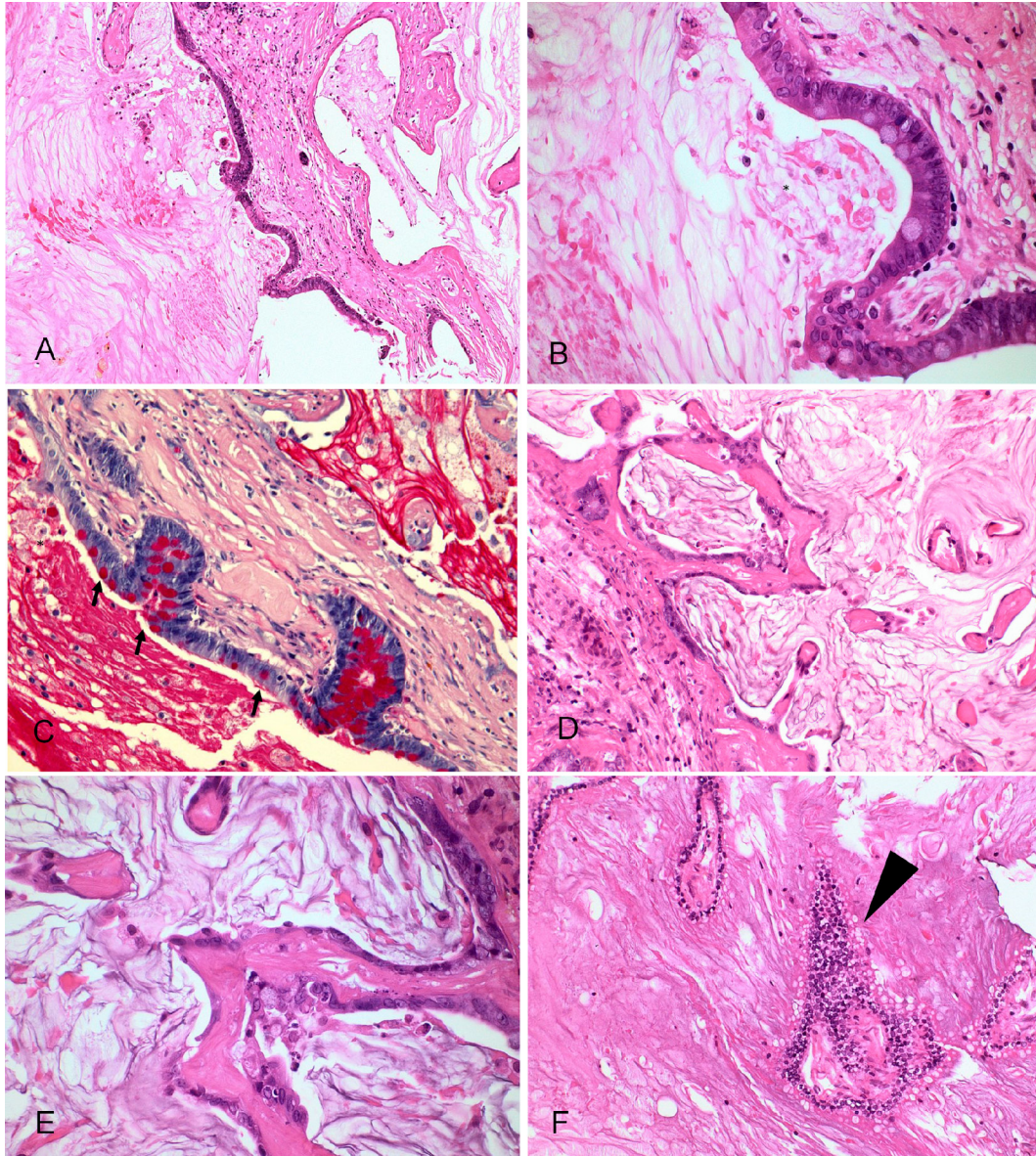


Fig. 2. Hematoxylin and eosin (A, B, D–F) and Periodic Acid-Schiff (C) staining of the cystic mass: (A) *Well-differentiated* cystic areas lined by a ciliated-cuboidal single cell to pseudostratified epithelium supported by a fibrovascular stroma. (B) At higher magnification, well-differentiated epithelium with goblet cells resembling Rathke's cleft epithelium. (C) Presence of PAS-positive Goblet cells (arrows). Keratin and mucus secretion stained pink. (D) *Poorly differentiated* neoplastic areas formed by irregular papillary projections with hyperkeratosis. (E) At higher magnification, papillary projections were lined by atypical squamous epithelium supported by fibrous stroma. (F) The multifocal occasional presence of spongy stratified epithelium. Magnification: (A) $\times 40$, (B) $\times 400$, (C) $\times 400$, (D) $\times 40$, (E) $\times 400$, (F) $\times 100$.

with RCCs combined with others compatible with CP. This observation supports that this hypothesis might also be true in rats. Further epidemiological investigations should be performed to determine if RCCs might predispose to CP; however, the high frequency of RCCs in humans²¹—in contrast with the rare appearance of CPs—speaks against this hypothesis.

In summary, RCCs and CPs are low-incidence background lesions that appear in rats and share some overlapping histological features due to their common origin from

Rathke's pouch epithelium. The present mass presented with well-differentiated areas compatible with RCC, admixed with poorly differentiated areas compatible with CP. These observations raise the suspicion of likely transition of RCC to CP, as it is believed to happen in humans.

Disclosure of Potential Conflicts of Interest: The authors declare no conflicts of interest. The author(s) received no financial support for the research, authorship, and/or publication of this article.

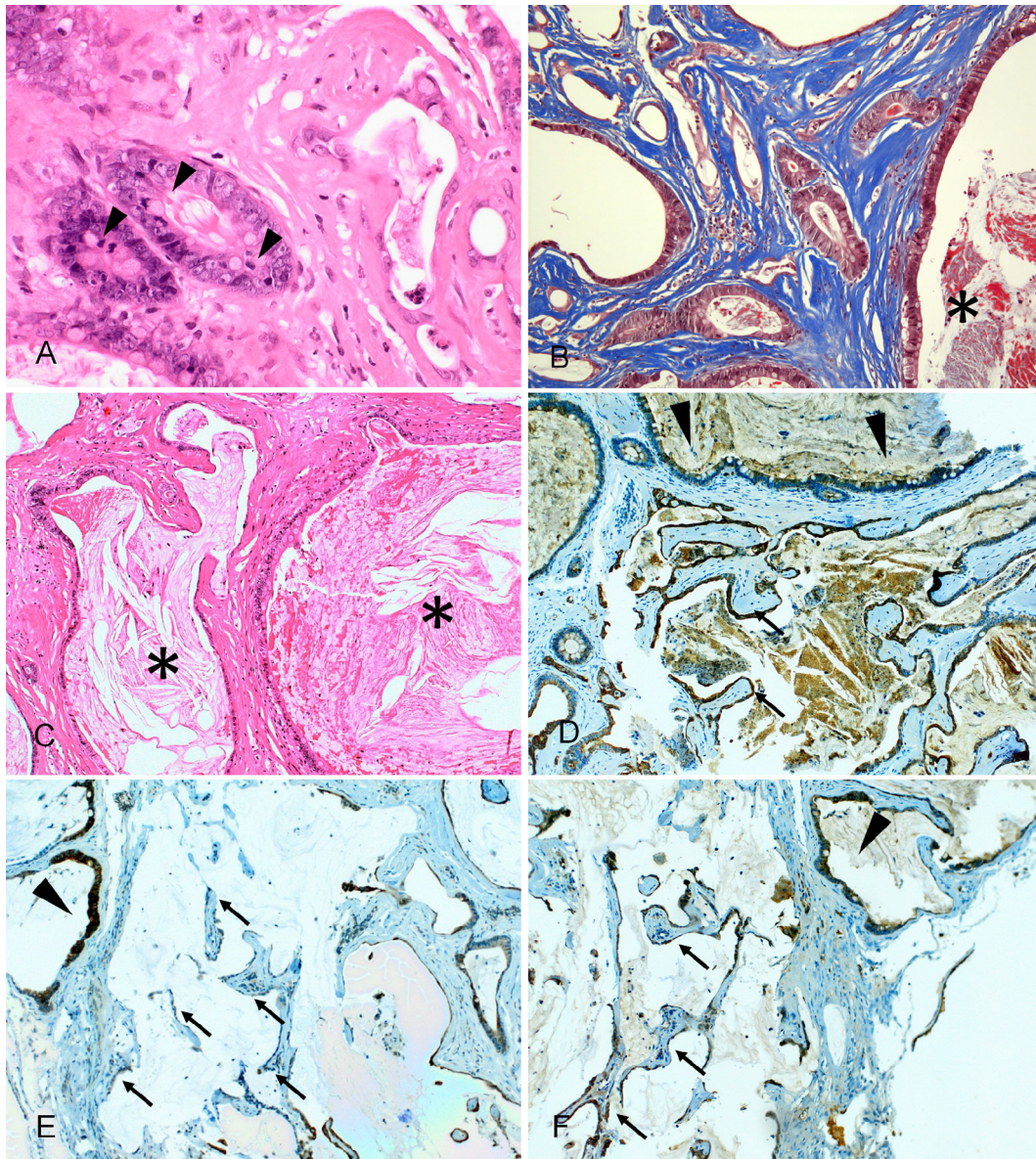


Fig. 3. Hematoxylin and eosin (A, C), Masson's Trichrome (B), and immunohistochemical staining against pancytokeratin (D), cytokeratin 20 (E) and cytokeratin 8 (F) of the mass in the pituitary gland. (A) Presence of mitotic figures (arrowheads). (B) Blue-stained fibrous stroma supporting the neoplastic epithelia. Mucus and keratin debris stain pale blue and red, respectively (asterisk). (C) Presence of abundant cholesterol clefts (asterisk) within cystic cavities. (D) Pancytokeratin immunohistochemistry showing positive immunolabeling of the keratin, single-cuboidal, well-differentiated epithelium (arrowheads) and of the atypical epithelium (arrows). (E) Cytokeratin 20 immunohistochemistry: Strong positive signal within the well-differentiated epithelium (arrowhead) in contrast with none to weak immunolabelling of the atypical areas (arrows) (F) Cytokeratin 8 immunohistochemistry: Positive immunostaining of well-differentiated epithelium (arrowhead), more variable in atypical areas (arrows). Magnification: (A) $\times 400$, (B) $\times 40$, (C) $\times 100$, (D–F) $\times 40$.

Acknowledgment: The authors thank Felix Weber and Nils Warfving for their critical review of the manuscript.

References

1. Brändli-Baiocco A, Balme E, Bruder M, Chandra S, Hellmann J, Hoenerhoff MJ, Kambara T, Landes C, Lenz B, Mense M, Rittinghausen S, Satoh H, Schorsch F, Seeliger F, Tanaka T, Tsuchitani M, Wojcinski Z, and Rosol TJ. Non-proliferative and proliferative lesions of the rat and mouse endocrine system. *J Toxicol Pathol.* **31**(3 Suppl): 1S–95S. 2018. [[Medline](#)] [[CrossRef](#)]
2. Maitra A. The endocrine system. In: Robbins and Cotran Pathologic Basis of Disease, 9th ed. (Robbins Pathology). V Kumar, A Abbas, and J Aster (eds). Elsevier Health Sciences, Philadelphia. 1073–1140. 2015.
3. Heinrichs M, and Ernst H. Spontaneous malignant craniopharyngioma in an aged Wistar rat. *J Toxicol Pathol.* **29**:

- 195–199. 2016. [[Medline](#)] [[CrossRef](#)]
4. Xin W, Rubin MA, and McKeever PE. Differential expression of cytokeratins 8 and 20 distinguishes craniopharyngioma from rathke cleft cyst. *Arch Pathol Lab Med.* **126**: 1174–1178. 2002. [[Medline](#)]
 5. Alomari AK, Kelley BJ, Damisah E, Marks A, Hui P, DiLuna M, and Vortmeyer A. Craniopharyngioma arising in a Rathke's cleft cyst: case report. *J Neurosurg Pediatr.* **15**: 250–254. 2015. [[Medline](#)] [[CrossRef](#)]
 6. Tateyama H, Tada T, Okabe M, Takahashi E, and Eimoto T. Different keratin profiles in craniopharyngioma subtypes and ameloblastomas. *Pathol Res Pract.* **197**: 735–742. 2001. [[Medline](#)] [[CrossRef](#)]
 7. Zada G, Lin N, Ojerholm E, Ramkissoon S, and Laws ER. Craniopharyngioma and other cystic epithelial lesions of the sellar region: a review of clinical, imaging, and histopathological relationships. *Neurosurg Focus.* **28**: E4. 2010. [[Medline](#)] [[CrossRef](#)]
 8. Schlaffer S-M, Buchfelder M, Stoehr R, Buslei R, and Hölsken A. Rathke's Cleft Cyst as Origin of a Pediatric Papillary Craniopharyngioma. *Front Genet.* **9**: 49. 2018. [[Medline](#)] [[CrossRef](#)]
 9. Iwata H, Hosoi M, Miyajima R, Yamamoto S, Mikami S, Yamakawa S, Enomoto M, Imazawa T, and Mitsumori K. Morphogenesis of craniopharyngeal derivatives in the neurohypophysis of Fisher 344 rats: abnormally developed epithelial tissues including parotid glands derived from the stomatodeum. *Toxicol Pathol.* **28**: 568–574. 2000. [[Medline](#)] [[CrossRef](#)]
 10. Park M, Lee S-K, Choi J, Kim S-H, Kim SH, Shin N-Y, Kim J, and Ahn SS. Differentiation between Cystic Pituitary Adenomas and Rathke Cleft Cysts: A Diagnostic Model Using MRI. *AJNR Am J Neuroradiol.* **36**: 1866–1873. 2015. [[Medline](#)] [[CrossRef](#)]
 11. Rottenberg GT, Chong WK, Powell M, and Kendall BE. Cyst formation of the craniopharyngeal duct. *Clin Radiol.* **49**: 126–129. 1994. [[Medline](#)] [[CrossRef](#)]
 12. Isobe K, Baily J, Mukaratirwa S, Petterino C, and Bradley A. Historical control background incidence of spontaneous pituitary gland lesions of Han-Wistar and Sprague-Dawley rats and CD-1 mice used in 104-week carcinogenicity studies. *J Toxicol Pathol.* **30**: 339–344. 2017. [[Medline](#)] [[CrossRef](#)]
 13. Martinez-Gutierrez JC, D'Andrea MR, Cahill DP, Santagata S, Barker FG 2nd, and Brastianos PK. Diagnosis and management of craniopharyngiomas in the era of genomics and targeted therapy. *Neurosurg Focus.* **41**: E2. 2016. [[Medline](#)] [[CrossRef](#)]
 14. Garnett MR, Puget S, Grill J, and Sainte-Rose C. Craniopharyngioma. *Orphanet J Rare Dis.* **2**: 18. 2007. [[Medline](#)] [[CrossRef](#)]
 15. Pace V, Heider K, Persohn E, and Schaetti P. Spontaneous malignant craniopharyngioma in an albino rat. *Vet Pathol.* **34**: 146–149. 1997. [[Medline](#)] [[CrossRef](#)]
 16. Fitzgerald JE, Schardein JL, and Kaump DH. Several uncommon pituitary tumors in the rat. *Lab Anim Sci.* **21**: 581–584. 1971. [[Medline](#)]
 17. Weber K, Garman RH, Germann P-G, Hardisty JF, Krinke G, Millar P, and Pardo ID. Classification of neural tumors in laboratory rodents, emphasizing the rat. *Toxicol Pathol.* **39**: 129–151. 2011. [[Medline](#)] [[CrossRef](#)]
 18. Kiupel M, Capen C, Miller R, and Smedley R. Histological classification of tumors of the endocrine system of domestic animals. Washington, DC: CL Davis DVM Foundation & Armed Forces Institute of Pathology; 2008.
 19. Rosol J, and Grone A. Endocrine glands. In: Jubb, Kennedy & Palmer's Pathology of Domestic Animals, Vol. 3, 6th ed. DJ Meuten (ed). Elsevier, St. Louis. 2016.
 20. Shin JL, Asa SL, Woodhouse LJ, Smyth HS, and Ezzat S. Cystic lesions of the pituitary: clinicopathological features distinguishing craniopharyngioma, Rathke's cleft cyst, and arachnoid cyst. *J Clin Endocrinol Metab.* **84**: 3972–3982. 1999. [[Medline](#)]
 21. Keyaki A, Hirano A, and Llena JF. Asymptomatic and symptomatic Rathke's cleft cysts. Histological study of 45 cases. *Neurol Med Chir (Tokyo).* **29**: 88–93. 1989.(in Japanese) [[Medline](#)] [[CrossRef](#)]
 22. Honegger J, Buchfelder M, Schlaffer S, Droste M, Werner S, Strasburger C, Störmann S, Schopohl J, Kacheva S, Deutschbein T, Stalla G, Flitsch J, Milian M, Petersenn S, Elbelt U. Pituitary Working Group of the German Society of Endocrinology Treatment of primary hypophysitis in Germany. *J Clin Endocrinol Metab.* **100**: 3460–3469. 2015. [[Medline](#)] [[CrossRef](#)]